# The technology, economy, and environmental sustainability of isotropic superfinishing applied to electron-beam melted Ti-6Al-4V components

The International Journal of Advanced Manufacturing Technology
https://doi.org/10.1007/s00170-021-07739-3

ORIGINAL ARTICLE

# The technology, economy, and environmental sustainability of isotropic superfinishing applied to electron-beam melted Ti-6Al-4V components

Eleonora Atzeni[1] · Angioletta R. Catalano[1] · Paolo C. Priarone[1] · Alessandro Salmi[1]

Received: 2 January 2021 / Accepted: 14 July 2021


**Abstract**
Additive manufacturing (AM) processes allow complex geometries to be produced with enhanced functionality, but technological challenges still have to be dealt with, in terms of surface finish and achieved tolerances. Among the consolidated powder-bed fusion processes, electron beam melting (EBM), which allows almost stress-free parts to be manufactured with a high productivity and minimum use of support structures, suffers from a poor surface quality. Thus, finishing processes have to be performed. The same geometrical complexity, which is considered one of the benefits of AM, becomes an issue when finishing is applied, in particular when internal features are present. Unconventional isotropic superfinishing processes could be a solution to this problem since they can generate a low surface roughness on complex geometries. However, the performance characteristics, with regard to the environmental sustainability and economic aspects, need to be evaluated since they are key factors that must be considered for decision-support tools when selecting a finishing process. The technological feasibility of the isotropic superfinishing (ISF) process, applied to Ti-6Al-4V parts produced by electron beam melting, is investigated in this paper by considering the dimensional and geometrical deviations induced by the finishing treatment, and from observations of the surface morphology. A significant reduction in surface roughness, $S_a$, to around 4 μm, has been observed on the most irregular surfaces, although the original shape is maintained. Environmental sustainability has been analyzed for all the manufacturing steps, from powder production to part fabrication, to the finishing process, and both the cumulative energy demand and material waste have been accounted for. The economic impact of the whole manufacturing chain has been evaluated, and the advantages of the ISF process are pointed out.

**Keywords** Sustainable manufacturing · Isotropic superfinishing · Additive manufacturing · Electron beam melting · Ti-6Al-4V

## 1 Introduction

It is generally considered that production is moving toward mass customization, and additive manufacturing (AM) technologies may be the key to satisfying both the customization and productivity demands. As regards metal production, the automation, control, and efficiency levels of AM systems have recently undergone rapid advances and are now considered a viable industrial production route. According to the Wohlers Report [1], the increasing number of metal AM system producers and metal AM system installations confirms this trend. AM systems allow for "digital production," since the parts are produced directly from their three-dimensional CAD models. Numerous advantages arise from this premise: the degree of geometrical complexity is the highest possible of all the production technologies, different functionalities can be combined in a unique component using a consolidation design, the material use can be optimized, and added value is gained. Despite these positive aspects, the surface quality and tolerances are quite low, and additional finishing operations may be needed. This is the case whenever close tolerances or high surface finishes are design requirements. Moreover, finishing treatments

✉ Paolo C. Priarone
paoloclaudio.priarone@polito.it

[1] Department of Management and Production Engineering, Politecnico di Torino, Corso Duca degli Abruzzi 24, 10129 Turin, Italy

Published online: 29 July 2021

are also required to improve fatigue performances, which are adversely affected by the inherent surface characteristics of metal AM parts.

Not all metal AM technologies result in the same surface properties. Basically, three consolidated AM technologies allow end-usable metal parts to be produced: laser powder bed fusion (L-PBF), electron beam powder bed fusion (EB-PBF), and directed energy deposition (DED). Of these, L-PBF parts may include intricate internal channels and present the lowest roughness and best accuracy, but they are also distinguished by high thermal gradients generated during the manufacturing process. Therefore, high residual stresses which limit the materials that can be processed are developed and the need for support structures and the adoption of specific design rules increases. Conversely, EB-PBF parts are almost stress-free, the productivity is higher than that of L-PBF, but the surface quality is poorer, and the high temperatures reached during the process (which cause the unmelted powder to form a partially sintered powder cake) limit the geometry of inlets, due to the difficulty of removing the internal powder. DED processes were the first technologies to be introduced onto the market, and they are excellent for repairing high-value parts; however, the surface finish is very rough and tolerances are large. Thus, machining operations are generally necessary. Essentially, the same opportunities of AM, in terms of geometrical complexity and material reduction, become a challenge when finishing processes are applied. If machining is adopted, difficulties arise in the holding and fixing parts in the machine, and the low stiffness may cause vibrations during machining and a loss of accuracy. Moreover, the cutting tool may find it difficult to reach intricate geometries. Unconventional finishing processes can be considered as an alternative.

Recent works in the literature have analyzed the finishing processes applied to metal AM parts. These processes can be classified according to their energy input, which may be chemical, electrochemical, thermal, or mechanical [2]. Chemical finishing processes have been tested successfully to remove unmelted powder particles from part surfaces and to polish internal and external features, as shown by Mohammadian et al. [3] and Tyagi et al. [4, 5]. However, the removal rate is very low and the process is thus particularly expensive. A higher removal rate can be obtained using electrochemical methods. A counter electrode is needed for electrochemical processes, and this limits the convenience of the method if the part includes internal geometries, especially complex narrow inlets [6–8]. Laser polishing is an ablation technique that can be integrated with L-PBF processes, in which building and polishing can be alternated [9, 10]. Among the mechanical processes, mass finishing processes can be considered very attractive, since they combine high productivity and low cost, as already demonstrated in several researches (such as Salvatore et al. [11]; Kumbhar et al. [10]; Atzeni et al. [12]; Ali et al. [13]). In these processes, the parts that have to be finished are placed in a tank and surrounded by an abrasive charge, that is, an abrasive medium with additives. The relative motion between the parts and abrasive particles allows part asperities to be removed, as a result of abrasion and plastic deformation mechanisms. On the other hand, the isotropic superfinishing (ISF) process is a chemically accelerated vibratory finishing technology that significantly increases the removal capability of the process, and thus the productivity. In the ISF process, a chemical compound reacts with surface peaks, thereby creating a coating film. The coating is constantly removed by the medium. Thus, the surface peaks are lowered and new unreacted material is exposed. As a result of such a removal mechanism, isotropic finishing can be considered non-directional. Even though the ISF process is suitable for finishing complex geometries [14], there is limited research work in the literature on its application to metal AM parts [15]. ISF is a complex process in which numerous process parameters interact together to result in the desired surface quality. These parameters include the frequency of vibrations, the selection and amount of the medium, the choice and dosing of the chemical accelerator, the material and surface characteristics of the part to be finished, and the cycle time. To date, the selection of optimal parameters is based on the operator's skills, and trial-and-error procedures are usually conducted [16].

In the past, post-processing operations relative to surface modification were investigated and optimized by evaluating their outcome almost exclusively on the basis of the part quality. However, in recent years, although the view through which analyzing and/or selecting a finishing process has expanded, a concurrent check on different aspects has become an established procedure. In particular, apart from the technological features, environmental and economic impacts have also begun to be included in the spectrum of characteristics of a process. In fact, the industrial sector exerts a key role in the global economy [17], as well as from the environmental viewpoint. On the one hand, the manufacturing sector uses significant amounts of energy, and this is also reflected on the energy market [18]. On the other hand, the climate change and the shortage of resources [19] make it necessary to undertake an urgent and responsible use of energy through more efficient and sustainable manufacturing processes. The energy efficiency problem is becoming increasingly important, and the need to decrease energy consumption in manufacturing has been evident for several years [20]. In the last decade, several efforts have been made in this direction [19]. Moreover, a life cycle assessment (LCA) can be a useful and exhaustive way of obtaining an awareness of the economic and environmental effects of a process. It allows the necessary material and energy resources to be quantified, as well as the released wastes and emissions, by identifying their flows along all the phases of a component's life cycle, from the production of the raw material to the end-of-life treatment

[21]. Böckin and Tillman [22] exploited an LCA to evaluate the implementation of the AM technology, based on powder-bed in the automotive sector, whereby they analyzed the production of metal parts of a light distribution truck engine, and compared this process with a conventional manufacturing one. Bekker and Verlinden [23] assessed three different processes while adopting a cradle-to-gate approach (green sand casting, CNC milling, and wire arc additive manufacturing) with the aim of increasing the knowledge on cleaner production systems through digital production. Ingarao et al. [24] compared forming, turning, and selective laser melting (SLM) processes for the production of aluminum parts. Zhang et al. [25] evaluated the energy consumption of a hybrid process (AM wire deposition plus micro-rolling), and compared it with the conventional manufacturing of wrought parts. Kellens et al. [26] reviewed the environmental dimensions of AM, for all the life cycle stages, including the utilization phase and the treatment of wastes. Ma et al. [19] considered energy consumption and the material costs for the optimization of the selecting laser sintering (SLS) process. However, to make manufacturing processes more sustainable, research should be addressed to energy consumption, costs, and the resource utilization rate [19]. Moreover, the idea of implementing economic and environmental factors in decision tools to select the most suitable finishing techniques, according to given design requirements, has already emerged in literature. Consumables and power consumption, together with safety implications, are factors that could be included in such process-selection frameworks, as could such information as the process speed and/or the level of integration of the post-processes within an AM chain [2].

EBM and ISF are commercially available technologies that are used in industry. However, companies still have to face technological challenges, in terms of both surface finishing and achieved tolerances. In this context, to the best of the authors' knowledge, few studies have addressed the isotropic superfinishing process after AM. Moreover, the review of the literature has (*i*) underlined the role of additive manufacturing-based integrated approaches in the sustainable development of industry and (*ii*) highlighted the need to simultaneously assess the technological, economic, and environmental life-cycle performance of such approaches. In order to fill these research gaps, the isotropic superfinishing process has been analyzed in this paper to assess its technological feasibility as well as the economic and environmental sustainability when applied to Ti-6Al-4V parts produced by electron beam melting. The technological feasibility of such a process has been investigated by identifying the dimensional and geometrical deviations induced by the finishing process at the desired surface finish value. Energy consumption, related to each step of the production cycle, from the raw material production to the final finished part, has been analyzed, and material waste has been accounted for. Finally, the economic impact of the finishing process has been evaluated. The materials and methods are detailed in Section 2. The results are presented and discussed with respect to (*i*) part quality, (*ii*) cumulative energy demand, and (*iii*) product costs in Section 3. The main conclusions are summarized in Section 4, and some insights into the research outlooks are given. The new experimental data and the empirical modeling framework presented in this study are aimed at filling the current research gaps and at providing a holistic methodology that can easily be replicated in other industrial research studies.

## 2 Materials and methods

In order to assess the feasibility of the finishing process, for both external and internal surfaces, a parallelepiped-shaped 50 × 50-mm$^2$ square cross section and 15-mm-high sample was designed with through holes of three different diameters, namely 15 mm, 10 mm, and 5 mm (as shown in Fig. 1). The choice of such a massive sample, which is characterized by a relatively simple geometry, does not allow the manufacturing complexity capabilities of AM to be fully exploited. However, it is expected that it will allow an accurate evaluation to be made of (*i*) the material flows, on a per-part basis, through the whole integrated manufacturing approach, as well as of (*ii*) the dimensional and geometric deviations induced by the finishing process. In this context, the choice of a simple mock-up, when evaluating the performance of post-AM finishing processes, is already established in the literature [27]. The production of the components, by means of electron beam melting (EBM), is described in Section 2.1, together with the post-AM operations. The procedures applied for the isotropic superfinishing (ISF) of the different part features are detailed in Section 2.2. The dimensional and geometrical characteristics have been measured according to Section 2.3. The environmental and economic impacts of the different unit processes have been quantified by applying the LCA-based analysis, presented in Section 2.4, under cradle-to-gate system boundaries.

### 2.1 Sample production

The samples were fabricated by an A2X system using Ti-6Al-4V ELI (Grade 23) gas-atomized powder with a particle size range from 45 to 105 μm, both of which were obtained from Arcam EBM. Ti-6Al-4V is an alloy that exhibits very high strength and excellent fatigue properties, high operating temperatures, low density, biocompatibility, and good corrosion resistance. It is widely used in the aerospace sector to satisfy the demand for lightweight components that are able to withstand highly static and dynamic loads, such as airframe structural components, gas turbines, and jet engines. The high biocompatibility of this alloy has led to its application being

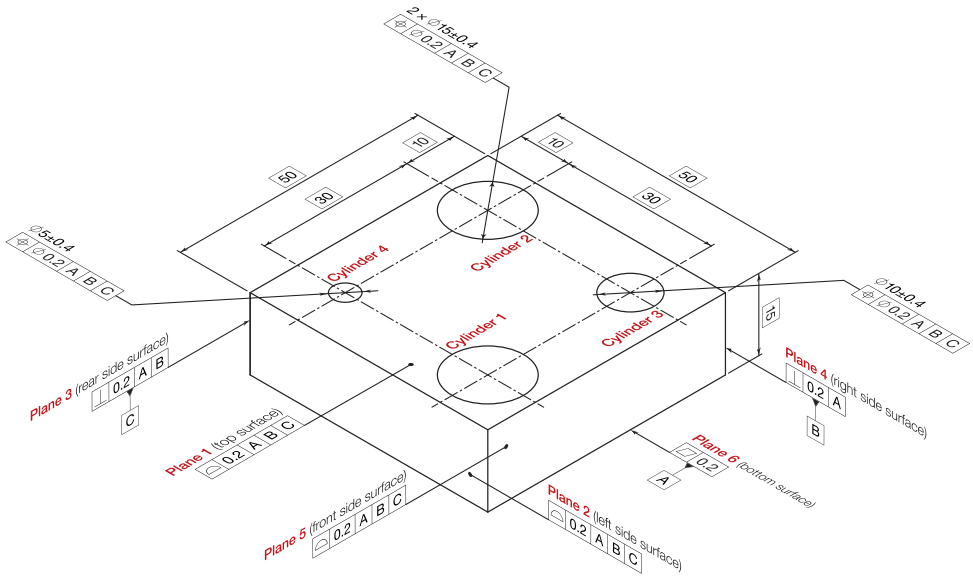


**Fig. 1** Geometry of the considered sample (dimensions in mm)

extended to the medical sector, where Ti-6Al-4V is used for implants, and to the marine and chemical industries, where a high resistance to corrosion is required [28]. The main limitation in the adoption of this material is related to its relatively high cost. The production of Ti-6Al-4V components by additive manufacturing is highly attractive, since cost-effective and optimized geometries can be obtained with a minimum waste. Table 1 lists the typical mechanical properties of Ti-6Al-4V parts produced by the EBM process.

EBM Control 5.0.64 software and the standard sets (themes) of process parameters for Ti-6Al-4V were adopted. The layer thickness was 50 μm, and the relevant process parameters for the "*Ti6Al4V A2X-PreHeat-50um-5.0.61*" and "*Ti6Al4V A2X-Melt-50um-5.0.61*" themes are listed in Table 2. Ten copies of the sample were produced, of which four were horizontally oriented (labeled as IDs 1 to 4), two copies were vertically aligned (IDs 9 and 10), and the other four were inclined by 45° with respect to the building direction (IDs from 5 to 8). In such a way, the different surface textures originated at different orientations by the EBM system were considered as a variable and analyzed in the experimental finishing campaign. Figure 2a shows the placement of

**Table 1** Mechanical properties of Arcam Ti-6Al-4V ELI (grade 23) [29]

| *Property* | *Value* |
|---|---|
| Modulus of elasticity | 120 GPa |
| Yield strength | 930 MPa |
| Ultimate tensile strength | 970 MPa |
| Elongation at breakage | 16% |
| Fatigue strength @ 600 MPa | > 10,000,000 cycles |
| Rockwell hardness | 32 HRC |

**Table 2** Main Ti-6Al-4V EBM process parameters of the Arcam EBM A2X system

| *Phase* | *Sub-phase* | *Process parameter* | *Value* |
|---|---|---|---|
| Pre-heating (50 μm) | Preheat 1 | Line order | 15 |
| | | Line offset | 1.2 mm |
| | | Focus offset | 62 mA |
| | | Hatch depth | 0.1 mm |
| | | Max beam current | 30 mA |
| | | Scan speed | 13,000 mm/s |
| | | Number of repetitions | 3 |
| | Preheat 2 | Line order | 15 |
| | | Line offset | 1.2 mm |
| | | Focus offset | 62 mA |
| | | Hatch depth | 0.1 mm |
| | | Max beam current | 38 mA |
| | | Scan speed | 14,600 mm/s |
| | | Number of repetitions | 3 |
| Melting (50 μm) | Contour | Scan speed | 850 mm/s |
| | | Focus offset | 6 mA |
| | | Beam current | 5 mA |
| | | Melting strategy | MultiBeam™ |
| | | Number of spots | 70 |
| | | Number of contours | 3 |
| | | Hatch contours | 0.29 mm |
| | Hatching | Speed function | 45 |
| | | Focus offset | 25 mA |
| | | Max beam current | 20 mA |
| | | Melting strategy | Continuous |
| | | Reference length | 45 mm |
| | | Reference current | 12 mA |
| | | Line offset | 0.20 mm |

the samples in the build envelope of the AM machine. The first layers in EBM Ti-6Al-4V part production (i.e., 2–3 mm along the building direction) are usually removed, since the fabricated parts may become deformed due to the distortion of the stainless-steel start plate. Moreover, as a result of the high temperatures of the building process, contamination may occur due to diffusion phenomena at the interface between the start plate and the fabricated parts. Thus, in the design of each specimen, the height was increased by a solid 3-mm-thick extruded support, to make allowances for the wire electrical discharge machining (WEDM) operation. The sample geometry of the angled sample was further modified by extending the planar surface to create a horizontal bottom plane. The excess material was then removed by WEDM. The added material (i.e., the solid support structures) is highlighted in red in Fig. 2a. The equipment used to remove the excess material was a CNC Wire Cut EDM DK7732 from Suzhou Baoma Numerical Control Equipment. The electrode was a molybdenum 0.18-mm-diameter wire. The pulse on-time was 33 μs, the pulse off-time was 4 μs, and the current and the machining voltage were set at "low" using the proprietary software of the WEDM machine.

## 2.2 REM isotropic superfinishing

The samples were subjected to a sandblasting process which, on average, lasted 20 min per part, in which a 60-mesh white corundum (aluminum oxide) was used. The REM isotropic superfinishing (REM ISF) process was then performed by means of a BF 100 BBSM vibro-finishing machine filled with 125 kg of FMX 15*15 ACT abrasive inserts. The process was executed in two subsequent steps of (*i*) finishing and (*ii*) polishing [15]. A commercial TIMIL medium, diluted 10:100 in water, was used in the finishing step, and the flow rate was fixed to 1 l/h. The finishing step lasted 48 h. This process was followed by a polishing step, in which an FBC 50 medium, diluted 1.5:100 in water, at a flow rate of 25 l/h, was used. The polishing step lasted 2 h. At the end of the vibro-finishing process, the specimens were extracted from the machine, washed in water, and dried.

## 2.3 Quality assessment

In order to retrieve geometrical and dimensional information, the samples were measured using a coordinate measuring machine (CMM), both before and after the finishing treatments. In such a way, it was possible to quantify any deviations induced by the building and finishing processes. An inspection was performed, in a controlled environment, through a DEA Global Image 07.07.07 CMM from Hexagon Manufacturing Intelligence, equipped with a PH10M indexable swinging head and an SP600 touch trigger probe (1-μm resolution), both from Renishaw. The machine has a volumetric measuring uncertainty, MPEE (maximum permissible error for length measurement), of 1.5 + $L$/333 μm, according to ISO-10360/2, as certified by the producer. A 2.0-mm-diameter probe tip was used to collect a total of 83 measurement points on the top and side surfaces of each specimen, and on the internal surfaces of the vertical holes. The edge length of the square cross section and the diameters of the holes were extracted from these data. The planarity of the top and side planes and the cylindricity of the holes were measured as regards the geometrical deviations. The data were then elaborated to compute any deviations induced by the EBM process with respect to the nominal CAD data and/or by the finishing treatment with respect to the actual EBM-ed geometry.

## 2.4 Economic and environmental impact assessment

The cradle-to-gate cost and the environmental footprint were assessed by accounting for the main contributions related to the powder production and all the manufacturing phases [24], as shown in Fig. 3. The cumulative energy demand (CED) was selected among the metrics usually considered for the environmental impact assessment, due to its ease of implementation and understanding [30]. The main material flows shown in Fig. 3 were measured experimentally. The weight of each sample and the related waste were quantified at each phase of the manufacturing cycle, using a

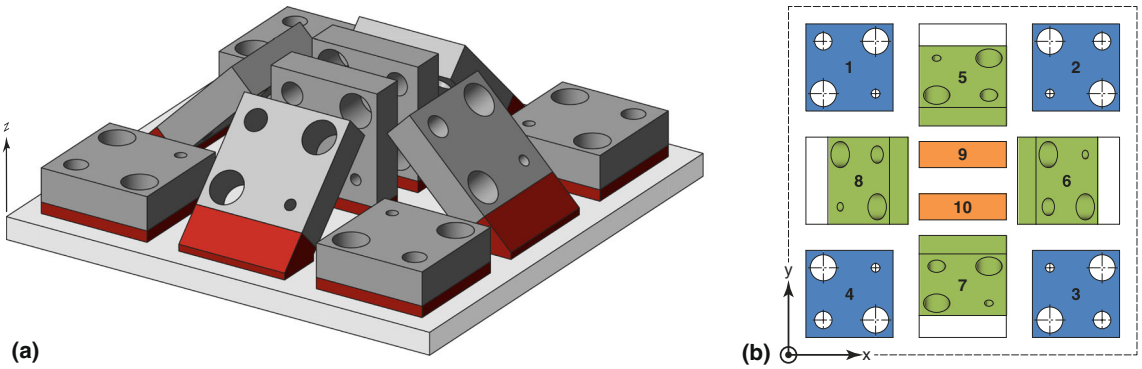


**Fig. 2** Placement of the samples in the build envelope of the AM machine (**a**) and their identification (ID) numbers (**b**)

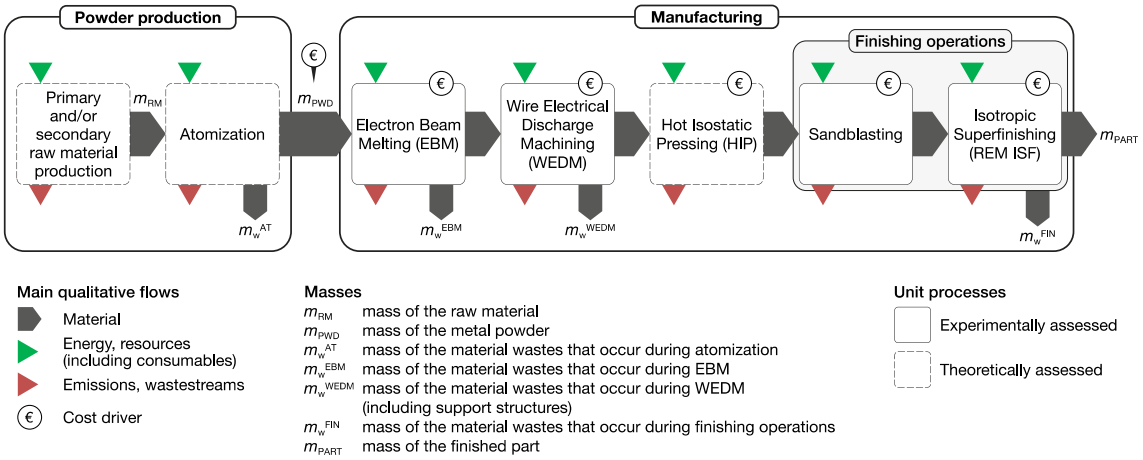


**Fig. 3** Cradle-to-gate boundaries for the assessment of the energy demand and costs

high-precision analytical weight scale from ORMA, to monitor the material losses. The weight scale sensitivity was 0.1 mg. A three-phase Fluke 430 Series II analyzer was used to characterize the electric energy consumption of the EBM and WEDM unit-processes, while including all the auxiliary apparatus (such as the EBM machine chiller). The "black-box" approach to process monitoring was followed during the analysis, even when the data regarding the finishing processes were provided by Best Finishing Srl. The data concerning the raw material production and the pre-manufacturing phases (i.e., the powder atomization) were extracted from the CES Selector database [31] or from the most recent literature sources. In addition, a hot isostatic pressing (HIP) was included in the economic and environmental assessment, even though it had not been experimentally performed, to verify whether its impacts could have been significant on the whole analysis.

## 3 Results and discussion

The results are presented and discussed hereafter with reference to the analyses carried out at the product level and process level. The results, in terms of dimensional deviations and surface quality of both the AM-ed and REM ISF-ed parts, are detailed in Section 3.1. Then, once the technological feasibility of the EBM + ISF integrated manufacturing approach had been verified, the results of the cradle-to-gate environmental (focusing on the cumulative energy demand) and economic assessment are given in Sections 3.2 and 3.3, respectively.

### 3.1 Part quality

Figure 4a shows the dimensional deviation of the additively manufactured samples with respect to the nominal dimensions, although limited to the edge length and hole diameters.

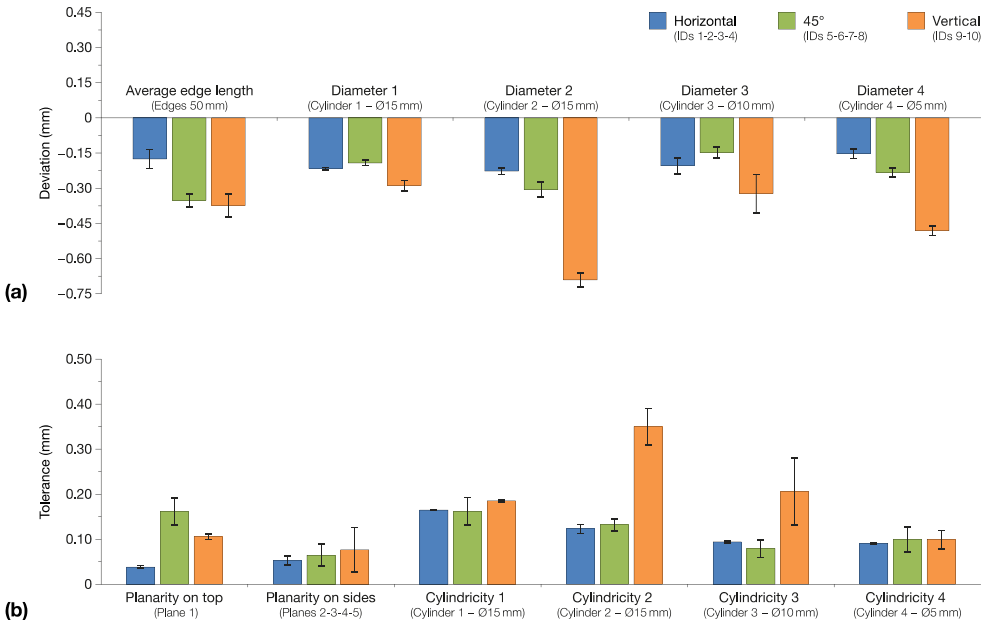


**Fig. 4** Effect of the part orientation on the dimensional deviations (**a**) and geometrical errors (**b**) in the as-built samples

The results are grouped considering the three orientations of the components inside the building volume. In general, the as-built parts were smaller than the nominal ones, since the scaling factors used to compensate for temperature shrinkage were not considered in the building preparation. As expected, better results were obtained for the horizontally aligned samples, with an average negative deviation of 0.20 mm. Larger deviations, around double the best case, were observed for the vertical orientation of the samples, with an average negative value of 0.43 mm. Intermediate results were obtained whenever the sample was inclined by 45° with respect to the building direction.

As regards the geometrical errors (shown in Fig. 4b), significant differences were only observed for "Plane 1," "Cylinder 2," and "Cylinder 3." "Plane 1" is horizontal for the IDs 1-2-3-4 samples (horizontal samples), and this led to a smoother and more precise surface. In this case, the deviation was about 0.04 mm. "Plane 1" is vertical for the IDs 9-10 samples (vertical samples), and the error rose to 0.10 mm. Finally, "Plane 1" is angled at 45° for the IDs 5-6-7-8 sample, and the error of 0.16 mm was the highest obtained for this feature. The large deviations observed on "Cylinder 2" and "Cylinder 3" are the direct consequence of the collapse of the hole and of the thermal effect/distortion at a higher distance from the platform, as these holes are positioned near the top of the built volume. In fact, the holes exhibited a form defect, as highlighted in the photograph in Fig. 5. Excluding these two features, the cylindricity errors were in general below 0.2 mm and independent of the sample orientation.

The deviations induced on the samples by the finishing operation (i.e., sandblasting plus REM ISF) are plotted in Fig. 6. As far as the dimensional deviation is concerned, the external edge length exhibited a reduction of up to 0.38 mm. Similarly, the hole diameters increased after finishing, with a greater effect being observed on larger holes. In general, a slightly higher removal was observed on the 45° samples, which were characterized by a more irregular surface (as highlighted in Fig. 7). The increase in the hole diameters suggests that the FMX 15*15 ACT abrasive medium and/or the chemical agent entered the holes during the process and removed material. No significant effect was found for the geometrical errors, which are comparable with those of the as-built samples.

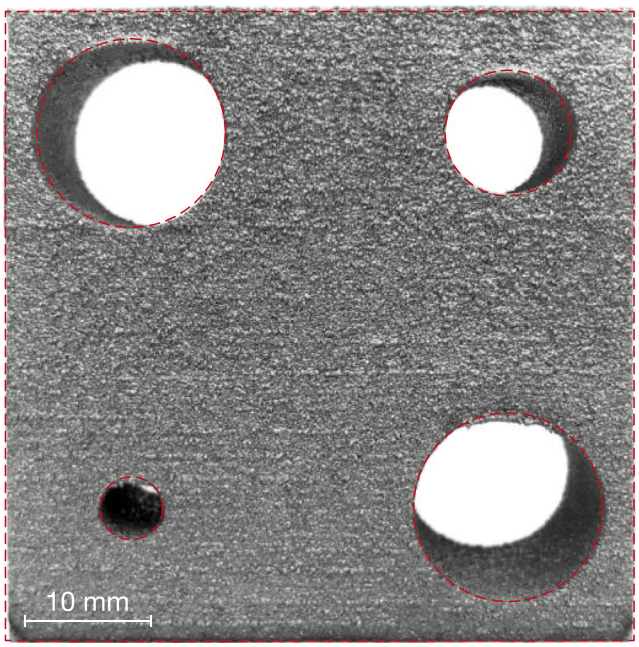


**Fig. 5** Form defect of the holes in the ID 6 sample (nominal geometry indicated with a red-dashed line)

Figure 7 shows bi- and tri-dimensional observations of the morphology of the (*i*) as-deposited, (*ii*) sandblasted, and (*iii*) REM ISF-ed surfaces (on "Plane 1") of a sample inclined by 45° with respect to the building direction. The sandblasting process leads to a significant reduction in the surface roughness parameters, while the changes in the surface morphology of the finished components are consistent with the typical ones of the chemically accelerated REM ISF process. The treatment is progressive, and the roughness is reduced by leveling the most exposed peaks, which results in the formation of an isotropic surface. The surface roughness parameters (computed in compliance with the ISO 25178 standard) are summarized in Table 3. A significant reduction in the $S_a$, $S_q$, $S_z$, $S_p$, and $S_v$ height parameters can be noted, compared with the results concerning the as-deposited samples. The surface skewness ($S_{sk}$) is slightly negative, and its value decreases with the increase in the duration of the finishing process, while the kurtosis ($S_{ku}$) and the areal material ratio ($S_{mr}$) parameters both increase slightly. Comparable results were obtained when REM ISF was applied to the additively manufactured samples made of aluminum [15].

The scale axis of the pictures has been adapted to better highlight the features of each surface.

### 3.2 Cumulative energy demand

The whole manufacturing approach was analyzed in view of its environmental and economic impact, once the technological feasibility of the REM ISF process to finish AM-ed components made of Ti-6Al-4V had been verified. The cradle-to-gate cumulative energy demand and the costs of producing the components (in Section 3.3) were the selected metrics. The primary energy was selected to quantify, at the same energy level, the different shares resulting from the resource/material flows and the electric energy flows, according to Frischknecht et al. [32]. The main critical flows of the energy, resources, and materials were accounted for. The life cycle inventory was acquired from an experimental characterization of each unit process, and it was extended, where needed, by including data obtained from the most recent literature. A primary-to-secondary energy conversion efficiency of 0.38 was

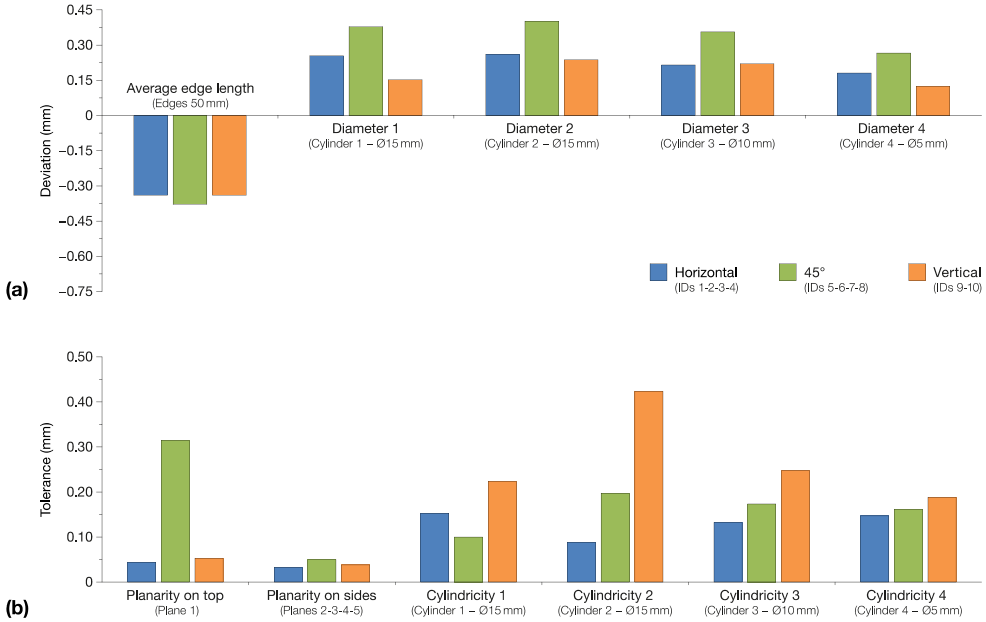


**Fig. 6** Effect of the part orientation on the dimensional deviations (**a**) and geometrical errors (**b**) after the finishing operations

considered [33]. Moreover, unless otherwise specified, a ± 10% range of variation was assumed for the input data collected from the literature to consider data uncertainty [30].

### 3.2.1 Powder production

The eco-properties of a cast, HIP-ed, and annealed alpha-beta Ti-6Al-4V alloy were extracted from the CES Selector 2017 database [31]. The embodied energy (i.e., the energy required to make 1 kg of the material from ores or feedstock) for the primary production of the raw material was 686.5 ± 5% MJ/kg. The benefit attained due to the upstream flow of recycled material was accounted for by using the "Recycled Content Approach" proposed by Hammond and Jones [34]. The energy for recycling and the recycled content in the actual supply were assumed to be 87.0 ± 5% MJ/kg and 22%, respectively [31]. As for the atomization process, Paris et al. [35] quantified the electric energy demand as 6.6 kWh per kilogram of titanium powder and the consumption of 5.5 $m^3$ of argon per kilogram. Considering these data, and assuming an embedded primary energy for argon production equal to 0.7 MJ/kg ([36], and references therein), the powder produced by atomization was here modeled by adding 68.8 ± 10% MJ/kg of embodied energy to that of the raw material production. As a result, the embodied energy of the Ti-6Al-4V powder was 623.4 ± 5.6% MJ/kg. Moreover, as the pre-manufacturing phase is included in the assessment, the powder atomization losses were estimated according to Paris et al. [35]. An input/output material ratio of 1.03 was assumed, and $m_{RM}$ (as labeled in Fig. 3) was quantified as 1666.7 g.

### 3.2.2 Electron beam melting

After loading the powder and setting up the machine, the EBM fabrication process consisted of three main phases: (*i*) the pre-process, (*ii*) the main process, and (*iii*) cooling down. The acquired power demand of the Arcam A2X EBM machine is plotted in Fig. 8 as a function of the processing time. The main sub-phases (namely: vacuum creation, machine calibration, heating, building, and cooling) and the related electric energy consumptions were quantified. The pre-process phase starts with the creation of an initial high vacuum in the building chamber and in the column. When a chamber pressure threshold of $5 \times 10^{-4}$ mbar is reached, the electron gun is ramped up. Simultaneously, the control vacuum system is activated: helium is introduced into the chamber and the gas flow is controlled in order to keep the average constant chamber pressure at $2 \times 10^{-3}$ mbar. A manual beam alignment is then performed. This procedure is required to tune the beam deflection (i.e., to reduce the position error of the beam) when different focus currents are used. Start plate heating is then performed for 30 min, in order to heat the start plate to 750 °C and realize a steady-state condition. At this point, the layer-wise building process starts. Each layer is processed in four steps: (*i*) powder spreading, (*ii*) dual-stage pre-heating, (*iii*) melting, and (*iv*) post-heating/post-cooling. Powder spreading is performed using a rake, and three passes are usually required, but the powder is fetched only once; more fetches (therefore more passes) are executed if the powder sensor identifies an underdosage. The freshly spread powder is then pre-heated to 750 °C using a defocused electron beam, adopting a dual-stage approach. In the first stage (*preheat 1*—PH1), a slight sintering of the powder bed is

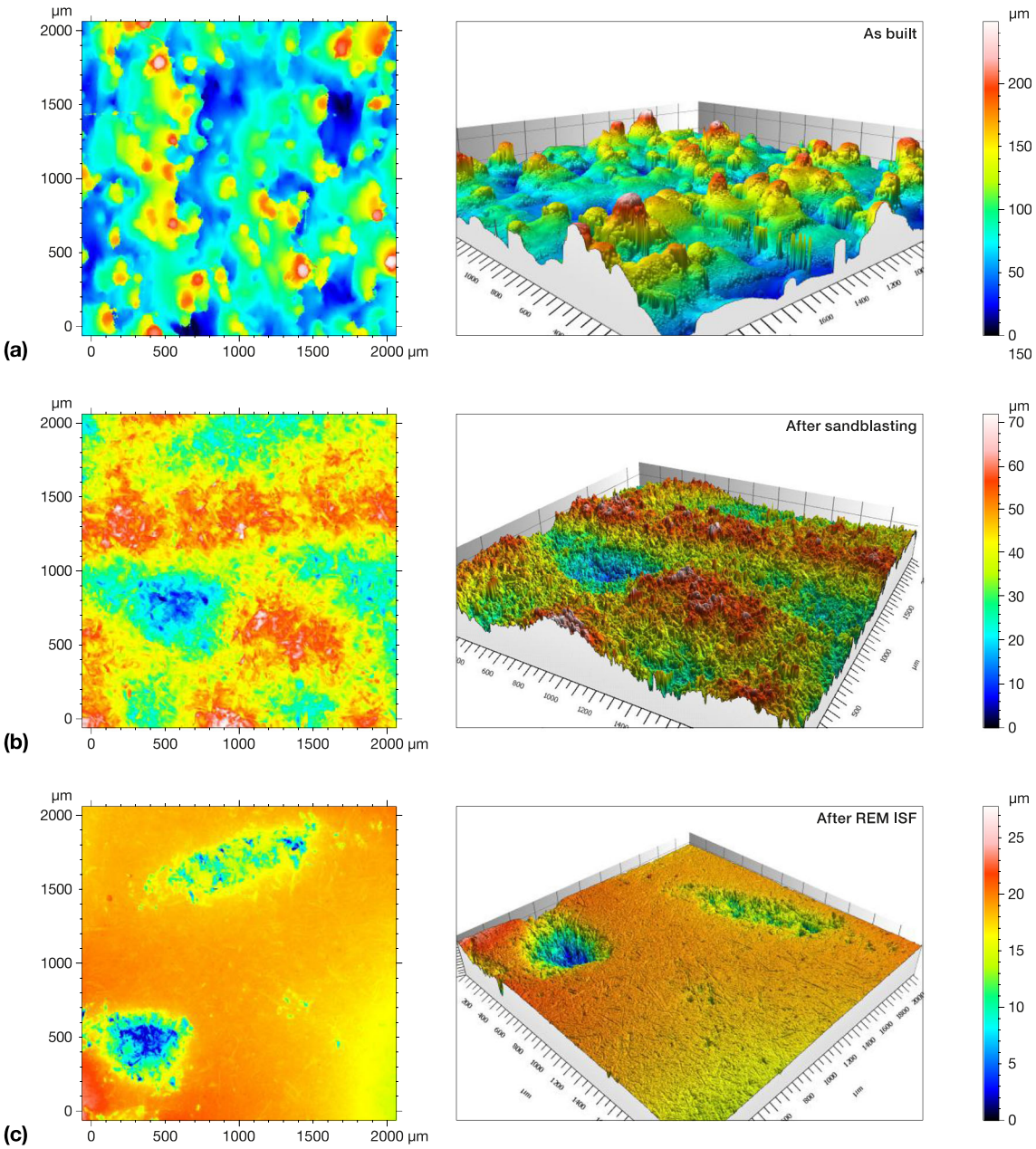


**Fig. 7** Bi- and tri-dimensional observations of the morphology of the as-built (**a**), sandblasted (**b**), and REM ISF-ed (**c**) ID 5 sample

performed across the bounding area surrounding all the parts; in the second stage (*preheat 2*—PH2), the preheated area follows the part contours, with an offset in order to increase the local sintering of the powder. In the melting step, the powder is selectively melted according to the bi-dimensional cross section computed during the slicing phase of the CAD data. The melting step is also performed in two stages, namely contouring and hatching. During the melting step, the EBM Control software evaluates the amount of energy transferred to the powder bed. A post-heating step is performed, if the transferred energy is not enough to keep the temperature of the powder bed constant; on the other hand, if the transferred energy causes an increase in the powder bed temperature, a post-cooling step is executed. The post-heating step is performed using the same process parameters as in the *preheat 1* step, while the post-cooling step involves a pause in the process (i.e., a few seconds, as computed by the control). The sequence of steps is then repeated at each layer until the built has been completed. The cool-down phase is started at the end of the process phase. The electron beam, all the servomotors, and the vacuum (turbo) pumps are switched off. Helium is then insufflated into the chamber to speed up the natural cooling down of the building chamber/fabricated parts while preventing oxidation. This last phase ends when the start plate reaches a temperature of 80 °C.

**Table 3** Typical surface roughness indices of the as-built and finished samples.

| | *Sample: horizontal* | | *Sample: 45°* | | *Sample: vertical* | |
|---|---|---|---|---|---|---|
| | *As-built* | *After finishing* | *As-built* | *After finishing* | *As-built* | *After finishing* |
| $S_a$ (μm) | 6.67 | 0.39 | 29.6 | 1.75 | 35.3 | 3.84 |
| $S_q$ (μm) | 8.46 | 0.74 | 37.8 | 2.78 | 43.6 | 6.42 |
| $S_z$ (μm) | 66.8 | 24.6 | 249 | 27.8 | 284 | 52.5 |
| $S_p$ (μm) | 33.2 | 11.7 | 162 | 10.1 | 134 | 10.9 |
| $S_v$ (μm) | 33.6 | 12.8 | 87.6 | 17.7 | 150 | 41.6 |
| $S_{sk}$ | 0.196 | − 4.8 | 0.733 | − 2.75 | 0.02 | − 2.76 |
| $S_{ku}$ | 3.50 | 45.00 | 3.48 | 12.20 | 2.68 | 12.40 |
| $S_{mr}$ (%) | 4.59 | 26.7 | 4.89 | 12 | 5.11 | 6.74 |

The total fabrication time was 26.4 h, which includes (*i*) a pre-process phase (machine setup, creation of an initial vacuum, beam alignment, and heating of the start plate), (*ii*) a process time of 17 h, and (*iii*) a final cool-down time. The total electric energy consumed for the production of the job was 74.0 kWh. The amount of deposited material ($m_{EBM}$, which accounts for the weight of the components, the support structures, and the allowances removed when finishing) was 1445.5 g; therefore, the specific electric energy consumption of the EBM machine, including the productive and non-productive times, was 184.3 MJ/kg. This value is coherent with the experimental characterization performed on the same AM machine by Lunetto et al. [37], and it is only slightly higher than the 61–177 MJ/kg range proposed by Kellens et al. [26] in their literature review. The average deposition rate, which was computed as the ratio of $m_{EBM}$ to the build time, was $8.5 \cdot 10^{-2}$ kg/h. The permanent material waste during the EBM process ($m_w^{EBM}$), which was due to the amount of non-reusable powder collected from the sieve and the Arcam Powder Recovery System (PRS), as well as to the powder trapped inside the holes of the components, was equal to 172.6 g (which can be spread equally over each

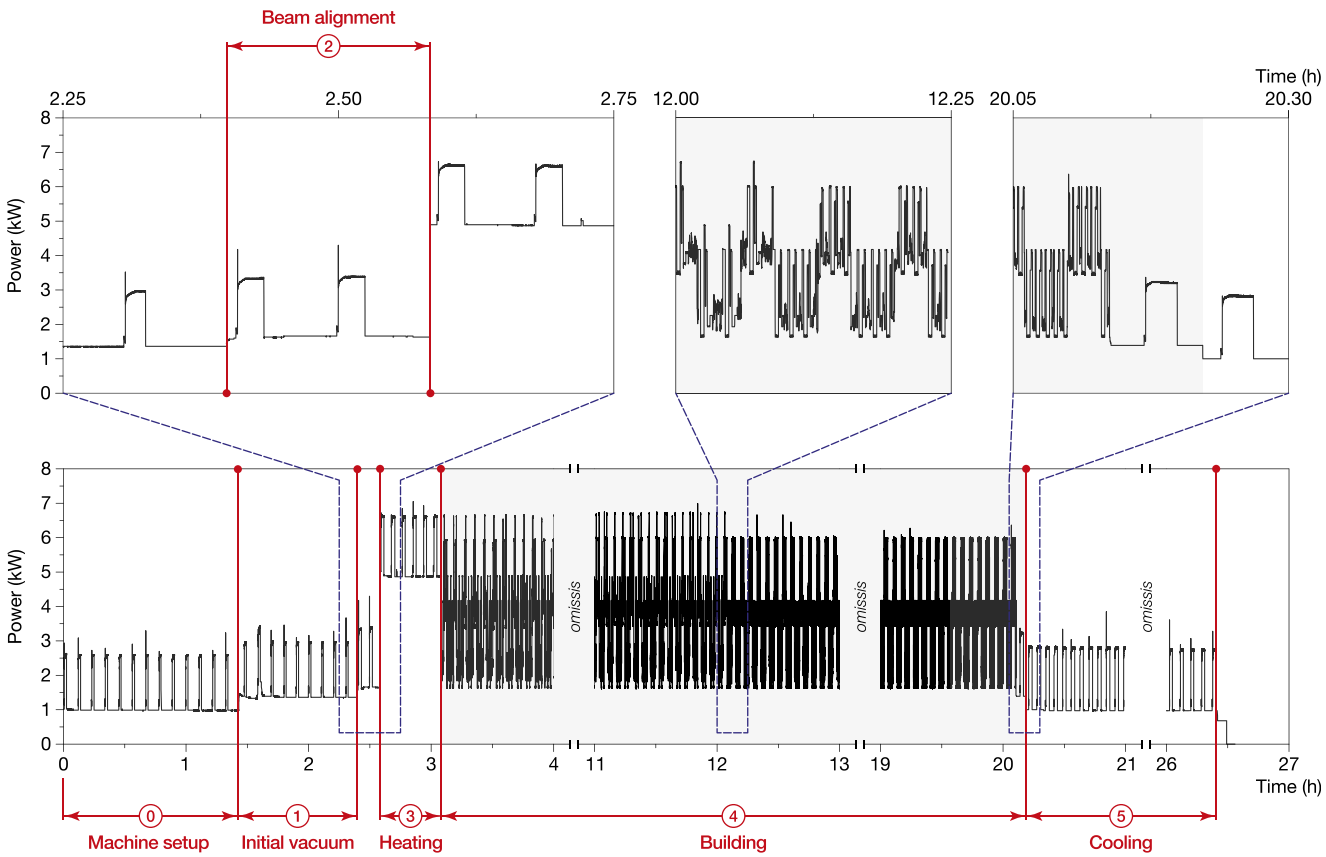


**Fig. 8** Power versus time profile acquired during the electron beam melting process

component). As a consequence, the powder mass ($m_{PWD}$) required to produce the job was 1618.1 g. The total consumption of helium was quantified as 92 l (at atmospheric pressure). Therefore, if the specific amount of energy of 0.4 to 0.7 kWh/m$^3$, as quantified by Liemberger et al. [38] for the production of helium (by extraction from natural gas) with 99.9% (v/v) at 25.81 bar is assumed, the contribution of its consumption to the CED appears to be negligible in the present research. Therefore, the experimentally obtained specific primary energy consumption of the whole EBM-unit process was 485.0 MJ/kg of deposited material.

#### 3.2.3 Post-AM processes

The support structures were removed by means of the wire-EDM process. The resulting flow of wasted material ($m_w^{WEDM}$) was 316.9 g, of which 97.3% was made up of the mass of the supports, whereas the metal particles deriving from WEDM cutting contributed to a lesser extent. As for the EBM process, the energy requirements of WEDM were measured experimentally. Figure 9 shows, as an example, the power demand versus time curve acquired when the support structures were removed from the two components labeled ID 5 and ID 6, since all the parts were cut into pairs to optimize the setup times. The results, in terms of electric energy consumption and total process time (including the setup), are summarized in Table 4, and refer to each manufactured part. The cutting time increased when the WEDM-ed cross section increased, as the machine automatically reduced the wire feed speed from 1.7 to 1.9 mm/min (for IDs 5 to 10) to 0.9 mm/min (for IDs 1 to 4). An average setup time of 0.12 h was assumed for each component, in order to account for the clamping and unclamping operations. Considering all the tests, the specific electric energy consumption necessary to cut a unit area of surface (including both the cutting and the setup phases) was evaluated to be within $0.34 \times 10^{-3}$ and $0.61 \times 10^{-33}$ kWh/mm$^2$ range. The contributions of the consumables (i.e., due to the wire and the dielectric consumption) were assumed to be negligible on a per-part basis. In addition, a hot isostatic pressing (HIP) was theoretically included in the assessment, to verify whether its impacts could be significant on the whole analysis. A specific primary energy demand of 122.0 ± 10% MJ/kg was obtained for the HIP of Ti-6Al-4V by referring to the data of Laureijs et al. [39].

**Table 4** Average and range values for the electric energy demand and process time of WEDM.

| *Growth direction* | *Electric energy (kWh)* | *Time (h)* |
|---|---|---|
| Horizontal (IDs 1–2–3–4) | 0.69 [0.66–0.71] | 1.01 [0.97–1.03] |
| 45° (IDs 5–6–7–8) | 0.41 [0.35–0.45] | 0.62 [0.54–0.67] |
| Vertical (IDs 9–10) | 0.36 [0.36–0.37] | 0.56 [0.55–0.56] |

#### 3.2.4 Finishing processes

All the AM-ed components were subjected to a sandblasting operation, followed by REM isotropic superfinishing. The energy consumption of the sandblaster should be addressed to (*i*) the power demand of the machine equipment (such as the grain recovery system and the filtering and dust treatment system) and (*ii*) the production of compressed air (CA). CA systems can have a significant impact on the energy efficiency of manufacturing plants. The air consumption of the sandblaster is mainly related to the diameter of the nozzle and the exerted pressure. The capacity of air supplied under pressure (awry of the nozzle) of 6 bar through a 5-mm-diameter nozzle was estimated to be in the 1.2 to 1.6 m$^3$/min range. Therefore, assuming (*i*) a 2-kW-rated sandblaster and (*ii*) the specific energy consumption of an industrial CA generation system within the 0.12–0.13 kWh/m$^3$ range (according to the simulation model proposed for FSD and VSD compressors by Mousavi et al. [40]), the resulting primary energy demand for the sandblasting operation (lasting 20 mins) could range from 33.6 to 45.7 MJ per part. It is worth remarking that comparable results can be obtained by applying the rule of thumb for which each horsepower (HP) of the sandblaster's compressor yields approximately 100 l/min of rendered air. The hourly consumption of the sandblaster's abrasive medium depends on several factors and is hard to quantify in a short-term experimental trial. However, the adoption of suction blasters that allow the used abrasive material to be collected and in general to be re-used, together with the low embodied energy of corundum (< 10 MJ/kg, according to Kirsch et al. [41]), made this contribution to CED negligible.

The BF 100 BBSM vibro-finishing machine which was used to perform the REM isotropic superfinishing required a constant power demand of 0.75 kW. The process (including both the finishing and polishing steps [15]), lasted 50 h, and 50 parts were estimated to be simultaneously treated for each finishing cycle. This results in an electric energy consumption of 2.7 MJ/part. The specific consumption of the FMX 15*15 ACT abrasive inserts was quantified as 0.08%/h, with a total consumption of 0.1 kg of abrasive medium per part. The total consumption of TIMIL TI-250 and FBC 50 was 4.80 kg and 0.75 kg, respectively, thus resulting in a consumption per part of 0.096 kg/part and 0.015 kg/part. The chemical reactants are made of a blend of different substances (such as sulfonamide acid, ammonium hydrogenodifluoride, hydrogen peroxide, 3-sodium nitrobenzene sulfonate, et cetera). Therefore, the environmental concerns that are associated with their preparation and use are connected more closely to liquid and hazardous waste than to the energy/resource consumption here considered. Therefore, this suggests the need of an extension of

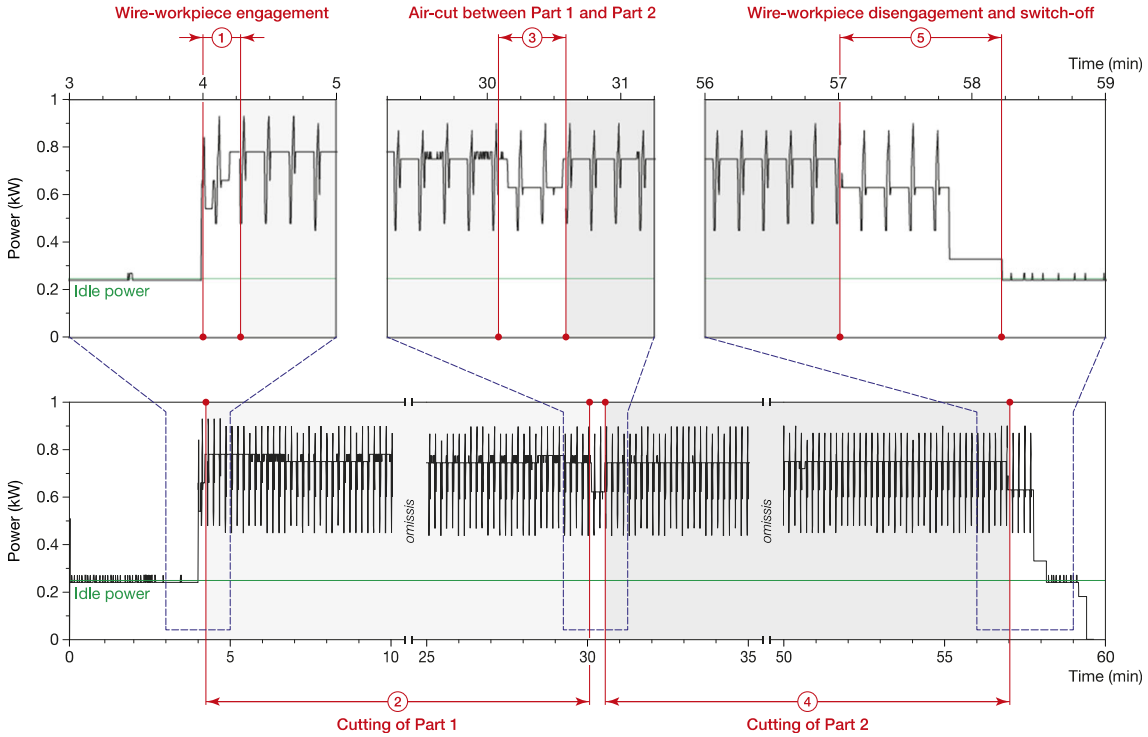


**Fig. 9** Power versus time profile acquired during wire-electrical discharge machining

the research, while accounting for different LCA impact categories [42]. The material losses resulting from the finishing operations (performed through two successive sandblasting and ISF phases) were calculated as the difference between the weight of the incoming component and that of the finished one, which resulted to be below 5 g/part.

### 3.2.5 CED: main results

Figure 10 summarizes the main material flows and the CED as functions of the orientation of the component inside the build volume of the machine. The stacked-bar graphs show the values computed by averaging the results of the equally oriented components, while the error bars quantify the minimum-to-maximum variability range. The weight of the finished components in Fig. 10a is almost uniform (approximately 110 g), whereas the weight of the support structures varies with respect to the direction of growth, and is slightly higher for the horizontal- and 45°-oriented samples. This result affects the CED values (Fig. 10b), due to the higher energy content embedded in the raw material needed for each part. The energy shares highlight a prevalent effect of the powder production phase (even though the benefits of the incoming recycled material are considered), which is followed by the energy consumption of the EBM process and the subsequent finishing operations. The energy demand, due to the production of CA for the sandblaster, in particular cannot be neglected. This is likely due to the manual sandblaster considered in this trial, which requires a long process time. The use

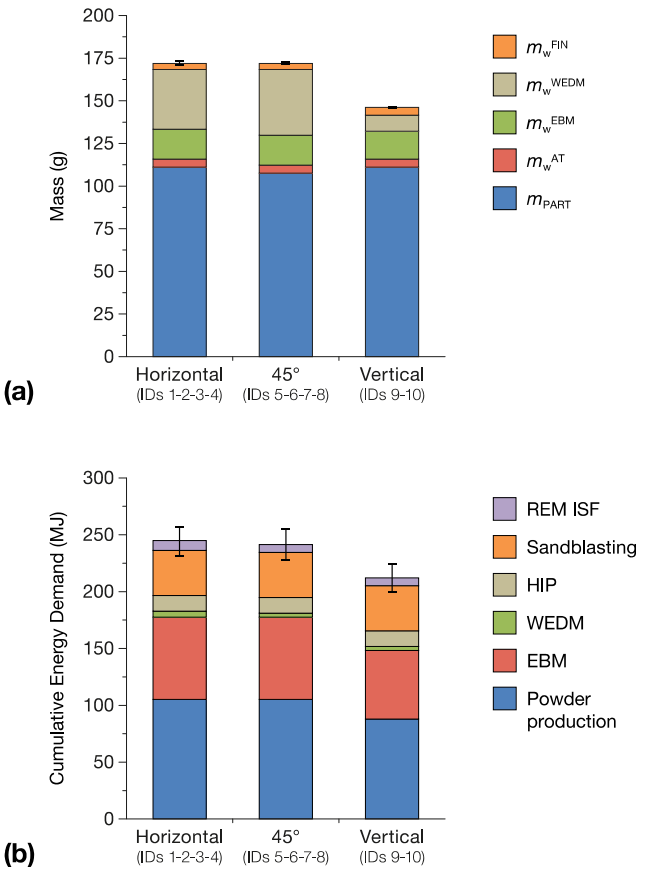


**Fig. 10** Material consumption (**a**) and CED (**b**) per produced part as a function of the orientation of the component

of automated sandblasting systems, which are already available on the market and are capable of simultaneously treating multiple parts, could reduce the time and costs of this operation. Moreover, the impact of the finishing process on the AM-ed parts deserves a digression. REM ISF, coupled with a preliminary sandblasting process, has proved to be technologically feasible. Nonetheless, the total primary energy required for the two unit-processes appears to be higher than that of other finishing processes, such as conventional milling. In fact, the finish machining of a Ti-6Al-4V can be rated as 22.1 (± 5%) MJ per kg of removed chips [43]. Therefore, the energy efficiency of alternative finishing processes (such as REM ISF) should be better quantified when complex internal/external geometries (which are not easily obtainable with traditional material removal tools) have to be produced.

## 3.3 Economic assessment

The manufacturing cost per produced part was computed as the sum of (*i*) the direct material costs, (*ii*) the direct labor costs, and (*iii*) the manufacturing overhead (MOH) costs, under the assumptions detailed in the following paragraphs. The cost assessment was performed on a per-part basis, regardless of the production volumes.

### 3.3.1 Direct material costs

The purchase costs of the incoming feedstock material (i.e., the metal powder for the EBM machine) was quantified as 175 € per kg of Ti-6Al-4V powder, according to Ingarao and Priarone [33]. This cost, which is driven by market rules, was assumed to vary within a ± 10% range, in order to account for market fluctuations. Direct material costs were allocated to each produced part, depending on the amount of required powder (which is shown in Fig. 10a).

### 3.3.2 Direct labor costs

The direct labor costs were computed by multiplying the labor charge rate by the working time of the machine operator(s). A mean nominal hourly labor cost (including wages/salaries, taxes, social contributions, et cetera) for an Italian specialized technician of 24.9 €/h (± 10%) was considered, on the basis of the data provided by the Italian Ministry of Labour and Social Policies [44]. It was assumed that all the operators involved in the whole manufacturing chain were at the same wage level. The working time for the EBM process was quantified as 4 h of working time (i.e., 2 operators working 2 h each during the machine setup and cleaning operations), which results in 0.4 h/component. Moreover, the working times for the WEDM, sandblasting, and REM ISF processes were 0.12, 0.33, and 0.02 h/component. With the sole exception of the sandblasting process, which was manually carried out, all the other automated processes mainly required operators for the handling, loading, and unloading of the (semi-)finished parts, with a minimum amount of time dedicated to supervision activities. Downtimes related to logistics and the movement of materials and parts between the unit-processes were not considered in the boundaries of the analysis (according to Section 2.4).

### 3.3.3 Manufacturing overhead costs

The manufacturing overhead costs include the manufacturing costs that are neither direct material costs nor direct labor costs. The depreciation and maintenance of the production equipment, and the costs of electricity and consumables were accounted for among the MOH costs. Other fixed factory-specific costs, such as the rent, insurance, and/or property taxes on plant facilities; the salaries paid to white collar workers, managers, and production floor supervisors; and other factory-related burdens were not included in the present assessment, since they can vary to a great extent, depending on the kind and size of the company. The assumed ranges for the machine cost rates (in €/h) are given in Table 5. The values were computed from the purchase costs of the equipment (which were obtained from an industrial market analysis) by assuming (*i*) a machine depreciation period of 8 years, and (*ii*) costs for maintenance and consumables equal to 5% of the machine purchase cost, per year [45]. The utilization rate for the EBM machine was adapted from the literature [36, 46], and the same assumptions were extended to the automatic REM ISF system. The utilization times for the sandblaster and the WEDM machine were estimated by assuming a working time of two or three 8-h shifts per day, over 220 working days per year. The cost of electricity was 0.15 ± 10% €/kWh, whereas a total specific cost of 10.9 ± 10% €/kg was considered for the HIP of Ti-6Al-4V (according to Ingarao and Priarone [33], who referred to the data of Laureijs et al. [39]).

**Table 5** Average and range values for the machine/equipment cost rates

| *Parameter* | *EBM* | *WEDM* | *Sandblasting* | *REM ISF* |
|---|---|---|---|---|
| Purchase cost of the machine/equipment (k€) | 900 [810–990] | 50 [40–60] | 20 [15–25] | 15 [10–20] |
| Utilization rate (%) | 62.5 [50.0–75.0] | 50.0 [40.0–60.0] | 50.0 [40.0–60.0] | 62.5 [50.0–75.0] |
| Utilization time (h/year) | 5475 [4380–6570] | 4400 [3520–5280] | 4400 [3520–5280] | 5475 [4380–6570] |
| Machine/equipment cost rate (€/h) | 28.8 [21.6–39.6] | 2.0 [1.3–3.0] | 0.8 [0.5–1.2] | 0.5 [0.3–0.8] |

### 3.3.4 Product costs: main results

The results, in terms of product costs (including direct material costs, labor costs, and manufacturing overhead costs), are plotted in Fig. 11. Overall, the stacked-bar graphs highlight that the few differences that can be observed in the average values for equally oriented components can be traced back to the different positioning of the component in the build volume of the AM machine. The wide minimum-to-maximum range of variability, which is quantified by the error bars, is due to the wide ranges of variation in the input data, as detailed above. For the here-considered components, the product cost is dominated by the manufacturing cost, where the cost of purchasing the Ti-6Al-4V powder is approximately one fifth of the total cost. Moreover, among the manufacturing costs, the cost of the EBM process ranges from 65 to 70% of the total product cost, and this is mainly due to the contribution of the manufacturing overhead costs (i.e., machine depreciation and its maintenance). These results are consistent with the available literature sources [24], regardless of the different cost modeling approaches that were reviewed in Costabile et al. [47]. The economic impact of the post-AM operations, which include WEDM, HIP, sandblasting, and REM ISF, accounts for less than 15% of the total. The finishing processes in particular deserve mentioning, and their cost results are detailed in Fig. 12. The cost of sandblasting dominates over all the finishing cost drivers. This is due to the contribution of the labor cost for the manually performed operations, which could be reduced by shifting to an industrially automated process. As far as the REM ISF process is concerned, half of the total cost originates from the costs related to the consumption of the abrasive inserts and the chemical media.

## 4 Conclusions and outlooks

Additive manufacturing has proved to be a disruptive technology within the Industry 4.0 framework since it provides new manufacturing solutions to several industrial sectors. The poor surface quality and the large tolerances of additive manufactured parts require post-AM finishing operations, and integrated additive-subtractive manufacturing approaches have to be planned. Finishing operations are usually performed via machining processes. However, the intrinsic complexity of the components produced through layer-by-layer fabrication often makes machining impractical, due to the difficulties the cutting tools have in obtaining all the features of intricate geometries as well as to the issues related to part clamping inside the working area of the machine tool. In such cases, alternative and unconventional finishing processes should be adopted.

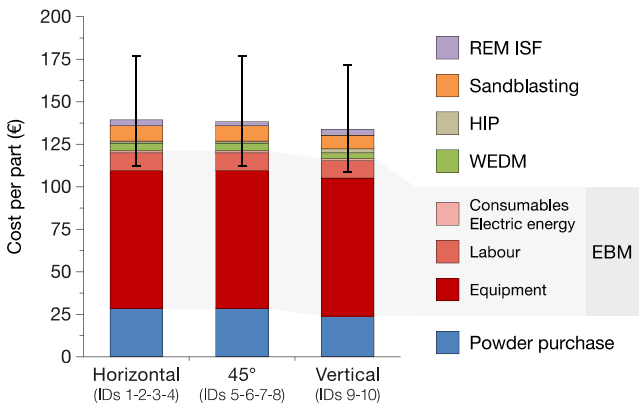


**Fig. 11** Results of the product costs under cradle-to-gate system boundaries

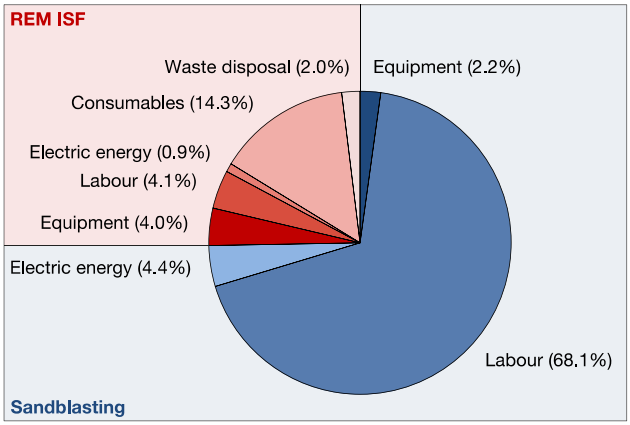


**Fig. 12** Cost results for the finishing operations (sandblasting plus REM ISF)

The finishing of electron-beam melted parts, by means of sandblasting followed by isotropic superfinishing, has been considered in this paper. Parallelepiped-shaped samples with through holes of different diameters were specifically designed to assess the feasibility of the finishing operations for both internal and external surfaces. The analyses were carried out at both (*i*) the product level, by comparing the dimensional deviations and surface quality results of EBM-ed and REM ISF-ed parts, (*ii*) and the process level, by performing a cradle-to-gate environmental and economic assessment. The resources and energy requirements of the different AM and post-AM unit-processes were experimentally characterized. Moreover, the study was conceptually extended to include the pre-manufacturing phase (for the powder production) and the HIP process, with the aim of quantifying all the contributions to the impact of the whole manufacturing chain.

As for the surface quality, the results prove the feasibility of the ISF process to enhance the surface quality of EBM-ed Ti-6Al-4V parts, by lowering the original surface roughness to $S_a \sim 4$ μm on the roughest planar surfaces, with a percentage decrease of about 90%. Since the orientation of the part during the EBM building process affects the surface quality of EBM, better results are obtained on horizontal surfaces, with a surface roughness of $S_a \sim 0.4$ μm, than on vertical surfaces. The

ISF process removes material by flattening the surface irregularities, and some material is removed while maintaining the original shape of the part and keeping the geometrical errors of the EBM-ed parts unchanged. The efficacy of the finishing of the internal features is limited by the mesh size of the abrasive particles, which cannot enter small-diameter holes. However, a certain degree of material removal has also been observed on the smallest internal features, mainly due to hatching caused by the chemical reactant.

As far as the cumulative energy demand is concerned, a prevalent effect of the powder production phase, which is due to the high embodied energy of the raw material, was noticed. The energy requirement of EBM was also relevant, because of the high specific energy consumption of AM, whereas the other subsequent post-AM unit processes contributed to a lesser (albeit non-negligible) extent. With reference to the here considered case study, few differences were observed concerning the orientation of the part within the build volume of the EBM machine. The lower the amount of the waste streams of the material is, the lower the CED, as expected. The product costs (including direct material costs, labor costs, and overhead manufacturing costs) were dominated by the costs related to manufacturing, and particularly by the EBM machine depreciation and its maintenance. The economic impact, due to all the post-AM operations (from WEDM to REM ISF), accounted for less than 15% of the total.

Overall, the REM ISF process was found to be suitable for finishing additively manufactured components made of a difficult-to-cut Ti-6Al-4V alloy. The treatment is progressive, and different surface quality results can be expected for different durations. The energy requirements and the costs of this finishing operation (even when including the manual sandblasting process) appear to be far lower than those of the other unit processes within the cradle-to-gate system boundaries. Nonetheless, the energy efficiency should be further verified, and compared with conventional machining, when much more complex geometries have to be produced. More importantly, the chemical composition of the reactants and the production of hazardous waste might affect different environmental impact categories, other than the CED that was assessed in this research. Therefore, further studies are needed to comprehensively address the sustainability of alternative finishing processes for additively manufactured parts.

**Acknowledgements** The Best Finishing Srl company is kindly acknowledged, and Marco Bonazzoli, Daniele Cataldo, and Gabriele Samadello in particular for the support provided in executing the experimental tests and in the assessment of the process costs. The authors also wish to thank Virginia Lo Schiavo for the contribution to this work during the development of her M.Sc. thesis in Engineering and Management at the Politecnico di Torino, and Sandro Moos for the support in defining the geometrical product specification and its tolerancing.

**Author contribution** E. Atzeni: investigation, writing—original draft, resources; A.R. Catalano: formal analysis, investigation; P.C. Priarone: methodology, formal analysis, writing—original draft; A. Salmi: visualization, resources, writing—review & editing.

**Funding** Open access funding provided by Politecnico di Torino within the CRUI-CARE Agreement. This research was partially supported by the "STAMP - Sviluppo Tecnologico dell'Additive Manufacturing in Piemonte" project, which was funded by the Piedmont Region (Italy) within the framework of POR-FESR, 2014-2020, as well as by the Interdepartmental Center for Integrated Additive Manufacturing IAM@PoliTo at the Politecnico di Torino (Italy).

**Availability of data and materials** The manuscript has no associated data. Data will be made available upon request.

## Declarations

**Competing interests** The authors declare no competing interests.

**Ethics approval** Not applicable.

**Consent to participate** Not applicable.

**Consent for publication** Not applicable.



## References

1. Wohlers TT, Campbell I, Diegel O, et al (2019) Wohlers Report 2019 - Additive manufacturing and 3D printing state of the industry
2. Gordon ER, Shokrani A, Flynn JM et al (2016) A surface modification decision tree to influence design in additive manufacturing. Smart Innov Syst Technol 52:423–434. https://doi.org/10.1007/978-3-319-32098-4_36
3. Mohammadian N, Turenne S, Brailovski V (2018) Surface finish control of additively-manufactured Inconel 625 components using combined chemical-abrasive flow polishing. J Mater Process Technol 252:728–738. https://doi.org/10.1016/j.jmatprotec.2017.10.020
4. Tyagi P, Goulet T, Riso C, Stephenson R, Chuenprateep N, Schlitzer J, Benton C, Garcia-Moreno F (2019) Reducing the roughness of internal surface of an additive manufacturing produced 316 steel component by chempolishing and electropolishing. Addit Manuf 25:32–38. https://doi.org/10.1016/j.addma.2018.11.001
5. Tyagi P, Goulet T, Riso C, Garcia-Moreno F (2019) Reducing surface roughness by chemical polishing of additively

manufactured 3D printed 316 stainless steel components. Int J Adv Manuf Technol 100:2895–2900. https://doi.org/10.1007/s00170-018-2890-0
6. Urlea V, Brailovski V (2017) Electropolishing and electropolishing-related allowances for powder bed selectively laser-melted Ti-6Al-4V alloy components. J Mater Process Technol 242:1–11. https://doi.org/10.1016/j.jmatprotec.2016.11.014
7. Urlea V, Brailovski V (2017) Electropolishing and electropolishing-related allowances for IN625 alloy components fabricated by laser powder-bed fusion. Int J Adv Manuf Technol 92:4487–4499. https://doi.org/10.1007/s00170-017-0546-0
8. Jung J-H, Park H-K, Lee BS, Choi J, Seo B, Kim HK, Kim GH, Kim HG (2017) Study on surface shape control of pure Ti fabricated by electron beam melting using electrolytic polishing. Surf Coat Technol 324:106–110. https://doi.org/10.1016/j.surfcoat.2017.05.061
9. Bhaduri D, Penchev P, Batal A, Dimov S, Soo SL, Sten S, Harrysson U, Zhang Z, Dong H (2017) Laser polishing of 3D printed mesoscale components. Appl Surf Sci 405:29–46. https://doi.org/10.1016/j.apsusc.2017.01.211
10. Kumbhar NN, Mulay AV (2018) Post processing methods used to improve surface finish of products which are manufactured by additive manufacturing technologies: a review. J Inst Eng Ser C 99:481–487. https://doi.org/10.1007/s40032-016-0340-z
11. Salvatore F, Grange F, Kaminski R, Claudin C, Kermouche G, Rech J, Texier A (2017) Experimental and numerical study of media action during tribofinishing in the case of SLM titanium parts. Procedia CIRP 58:451–456. https://doi.org/10.1016/j.procir.2017.03.251
12. Atzeni E, Barletta M, Calignano F, Iuliano L, Rubino G, Tagliaferri V (2016) Abrasive fluidized bed (AFB) finishing of AlSi10Mg substrates manufactured by direct metal laser sintering (DMLS). Addit Manuf 10:15–23. https://doi.org/10.1016/j.addma.2016.01.005
13. Ali P, Dhull S, Walia RS, Murtaza Q, Tyagi M (2017) Hybrid abrasive flow machining for nano finishing - a review. Mater Today Proc 4:7208–7218. https://doi.org/10.1016/j.matpr.2017.07.048
14. Gupta K, Jain NK, Laubscher R (2017) Conventional and advanced finishing of gears. In: Advanced gear manufacturing and finishing. Elsevier, pp 127–165
15. Atzeni E, Balestrucci A, Catalano AR, Iuliano L, Priarone PC, Salmi A, Settineri L (2020) Performance assessment of a vibro-finishing technology for additively manufactured components. Procedia CIRP 88:427–432. https://doi.org/10.1016/j.procir.2020.05.074
16. Nebiolo WP (2006) The basics of surface engineering by isotropic superfinishing (ISF) using a traditional vibratory finishing bowl. Proceedings of the National Association for Surface Finishing Annual Technical Conference 2006, SUR/FIN 2006. Milwaukee, Wisconsin, pp 43–52
17. Zhou L, Li J, Li F, Meng Q, Li J, Xu X (2016) Energy consumption model and energy efficiency of machine tools: a comprehensive literature review. J Clean Prod 112:3721–3734. https://doi.org/10.1016/j.jclepro.2015.05.093
18. Wippermann A, Gutowski TG, Denkena B, Dittrich MA, Wessarges Y (2020) Electrical energy and material efficiency analysis of machining, additive and hybrid manufacturing. J Clean Prod 251:119731. https://doi.org/10.1016/j.jclepro.2019.119731
19. Ma F, Zhang H, Hon KKB, Gong Q (2018) An optimization approach of selective laser sintering considering energy consumption and material cost. J Clean Prod 199:529–537. https://doi.org/10.1016/j.jclepro.2018.07.185
20. Zhong Q, Tang R, Peng T (2017) Decision rules for energy consumption minimization during material removal process in turning. J Clean Prod 140:1819–1827. https://doi.org/10.1016/j.jclepro.2016.07.084
21. ISO 14040 (2006) - Environmental management - life cycle assessment - principles and framework. https://www.iso.org/standard/37456.html. (Lastly accessed on May 3rd, 2021)
22. Böckin D, Tillman AM (2019) Environmental assessment of additive manufacturing in the automotive industry. J Clean Prod 226:977–987. https://doi.org/10.1016/j.jclepro.2019.04.086
23. Bekker ACM, Verlinden JC (2018) Life cycle assessment of wire + arc additive manufacturing compared to green sand casting and CNC milling in stainless steel. J Clean Prod 177:438–447. https://doi.org/10.1016/j.jclepro.2017.12.148
24. Ingarao G, Priarone PC, Deng Y, Paraskevas D (2018) Environmental modelling of aluminium based components manufacturing routes: additive manufacturing versus machining versus forming. J Clean Prod 176:261–275. https://doi.org/10.1016/j.jclepro.2017.12.115
25. Zhang H, Huang C, Wang G, Li R, Zhao G (2021) Comparison of energy consumption between hybrid deposition & micro-rolling and conventional approach for wrought parts. J Clean Prod 279:123307. https://doi.org/10.1016/j.jclepro.2020.123307
26. Kellens K, Baumers M, Gutowski TG, Flanagan W, Lifset R, Duflou JR (2017) Environmental dimensions of additive manufacturing: mapping application domains and their environmental implications. J Ind Ecol 21:S49–S68. https://doi.org/10.1111/jiec.12629
27. Atzeni A, Rubino G, Salmi A, Trovalusci F (2020) Abrasive fluidized bed finishing to improve the fatigue behaviour of Ti6Al4V parts fabricated by electron beam melting. Int J Adv Manuf Technol 110:557–567. https://doi.org/10.1007/s00170-020-05814-9
28. Srinivasan M, Ramesh S (2015) Synthesis and characterization of titanium alloy (Ti-6Al-4V) by high energy ball milling. Int J Appl Eng Res 10:11080–11084
29. Arcam AB, Ti6Al4V ELI titanium alloy (datasheet). www.arcam.com (Lastly accessed on May 3rd, 2021).
30. Ashby MF (2013) Materials and the environment: eco-informed material choice: 2nd edition. Elsevier Inc. Waltham and Kidlington: Butterworth Heinemann/Elsevier. ISBN: 978-0-12-385971-6.
31. CES Selector. (2017) v.17.2.0 database. Granta Design, the UK
32. Frischknecht R, Wyss F, Büsser Knöpfel S, Lützkendorf T, Balouktsi M (2015) Cumulative energy demand in LCA: the energy harvested approach. Int J Life Cycle Assess 20:957–969. https://doi.org/10.1007/s11367-015-0897-4
33. Ingarao G, Priarone PC (2020) A comparative assessment of energy demand and life cycle costs for additive- and subtractive-based manufacturing approaches. J Manuf Process 56:1219–1229. https://doi.org/10.1016/j.jmapro.2020.06.009
34. Hammond G, Jones C (2010) Inventory of carbon and energy (ICE), annex B: how to account for recycling; a methodology for recycling. The University of Bath, Bath
35. Paris H, Mokhtarian H, Coatanéa E, Museau M, Ituarte IF (2016) Comparative environmental impacts of additive and subtractive manufacturing technologies. CIRP Ann 65:29–32. https://doi.org/10.1016/j.cirp.2016.04.036
36. Kamps T, Lutter-Guenther M, Seidel C, Gutowski T, Reinhart G (2018) Cost- and energy-efficient manufacture of gears by laser beam melting. CIRP J Manuf Sci Technol 21:47–60. https://doi.org/10.1016/j.cirpj.2018.01.002
37. Lunetto V, Galati M, Settineri L, Iuliano L (2020) Unit process energy consumption analysis and models for electron beam melting (EBM): effects of process and part designs. Addit Manuf 33:101115. https://doi.org/10.1016/j.addma.2020.101115
38. Liemberger W, Miltner M, Harasek M (2018) Efficient extraction of helium from natural gas by using hydrogen extraction

technology. Chem Eng Trans 70:865–870. https://doi.org/10.3303/CET1870145
39. Laureijs RE, Roca JB, Narra SP, Montgomery C, Beuth JL, Fuchs ERH (2017) Metal additive manufacturing: cost competitive beyond low volumes. J Manuf Sci Eng Trans ASME 139:1–9. https://doi.org/10.1115/1.4035420
40. Mousavi S, Kara S, Kornfeld B (2014) Energy efficiency of compressed air systems. Procedia CIRP 15:313–318. https://doi.org/10.1016/j.procir.2014.06.026
41. Kirsch B, Effgen C, Büchel M, Aurich JC (2014) Comparison of the embodied energy of a grinding wheel and an end mill. Procedia CIRP 15:74–79. https://doi.org/10.1016/j.procir.2014.06.037
42. Dahmus JB, Gutowski TG (2004) An environmental analysis of machining. In: Proceedings of IMECE2004 ASME International Mechanical Engineering Congress and RD&D Expo, November 13-19, 2004. Anaheim, California, p 10
43. Priarone PC, Pagone E, Martina F, Catalano AR, Settineri L (2020) Multi-criteria environmental and economic impact assessment of wire arc additive manufacturing. CIRP Ann 69:37–40. https://doi.org/10.1016/j.cirp.2020.04.010
44. Italian Ministry of Labour and Social Policies (2018), D.D. 91/2018: Costo medio orario per il personale dipendente da imprese dell'industria metalmeccanica privata e della installazione di impianti. Available (in Italian) at www.lavoro.gov.it (Lastly accessed on May 3rd, 2021)
45. Baumers M (2012) Economic aspects of additive manufacturing: benefits, costs and energy consumption. Loughborough University
46. Baumers M, Dickens P, Tuck C, Hague R (2016) The cost of additive manufacturing: machine productivity, economies of scale and technology-push. Technol Forecast Soc Change 102:193–201. https://doi.org/10.1016/j.techfore.2015.02.015
47. Costabile G, Fera M, Fruggiero F, Lambiase A, Pham D (2017) Cost models of additive manufacturing: a literature review. Int J Ind Eng Comput 263–283. doi:https://doi.org/10.5267/j.ijiec.2016.9.001